Enhanced Photorefractive Performance and Optical Damage Resistance in Zirconium and Uranium Co-doped Lithium Niobate Crystals

*Tian Tian,[*a] Dong Zhang,[a] Tingfeng Wu,[a] Weiwei Wang,[b] Hongde Liu,[c] Dahuai Zheng,[c] Yaoqing Chu,[a] Hui Shen,[a] and Jiayue Xu [*a]*

[a] Institute of Crystal Growth, School of Materials Science and Engineering, Shanghai Institute of Technology, Shanghai 201418, China.

[b] Shijiazhuang Tiedao University, Shijiazhuang, 050043, China

[c] MOE Key Laboratory of Weak-Light Nonlinear Photonics, School of Physics and TEDA Institute of Applied Physics, Nankai University, Tianjin 300071, China.

*E-mail: tiant@sit.edu.cn; xujiayue@sit.edu.cn.

Contents

Doping concentration selection

A congruent LN:Zr,U crystal with a Li/Nb ratio of 48.38/51.62 was grown. Based on the Li-vacancy defect model, the intrinsic non-stoichiometry results in approximately 3.2 mol% Nb antisite defects (Nb_{Li}^{4+}). According to the expression of Eq. (1), it could be seen that the removal of 3.2 mol% original Nb_{Li}^{4+} defects exist in LN requires 1.28 mol% ZrO_2.

$$2ZrO_2 + 5\left(V_{Li}\right)_{4/5}\left(Nb_{Li}^{4+}\right)_{1/5}NbO_3 + 2LiNbO_3 = 8\left(Zr_{Li}^{3+}\right)_{1/4}\left(V_{Li}^{-}\right)_{3/4}\left(NbO_3\right)_2 + 2Li_2O \quad (1)$$

$$6LiNbO_3 + UO_3 = \left(V_{Li}^{-}\right)\left(U_{Nb}^{+}\right)O_3 + 5\left(V_{Li}^{-}\right)_{4/5}\left(Nb_{Li}^{4+}\right)_{1/5}NbO_3 + 3Li_2O \quad (2)$$

$$2ZrO_2 + UO_3 + 8LiNbO_3 = \left(V_{Li}^{-}\right)\left(U_{Nb}^{+}\right)O_3 + 8\left(Zr_{Li}^{3+}\right)_{1/4}\left(V_{Li}^{-}\right)_{3/4}\left(NbO_3\right)_2 + 3Li_2O \quad (3)$$

Assume that all U^{4+} were oxidized to U^{6+} to occupy the Nb site during the estimation, a large number of Nb_{Li}^{4+} would be introduced in LN, which could be expressed in the formula of Eq. (2). According to the formula of Eq. (3), if 0.6 mol% U is doped into LN, the ZrO_2 concentra-tion required to remove these Nb_{Li}^{4+} defects generated by doping U ions could be calculated to be 1.2 mol%. Therefore, the estimated threshold concentration of Zr is 2.48 mol%. It should be noted that this threshold concentration was estimated based on a simplified charge compensation model and is used only for threshold analysis. In this estimation, all U^{4+} ions were assumed to be oxidized to U^{6+} in order to obtain the theoretical upper limit estimate, thereby providing a practical basis for selecting the dopant concentration range. Therefore, the value obtained here should be regarded only as an approximate estimation rather than an exact threshold concentration.

Solid state synthesis

A series of LN:Zr,U crystals with a diameter of 1 inch were grown by an improved Bridgman method. On the basis of the previous work, fixed the UO_2 doping amount at 0.6 mol%. Selected the ZrO_2 concen-tration of 1.0, 3.0, and 4.0 mol% and the composition of Li/Nb = 48.38/51.62, marked as LN: $Zr_{1.0}$,U, LN: $Zr_{3.0}$,U and LN: $Zr_{4.0}$,U respectively. Nb_2O_5, Li_2CO_3, UO_2, and ZrO_2 (all 99.99% purity) were used as starting materials. For polycrystalline feedstock preparation, Nb_2O_5 was first annealed at 800℃ for 5h to remove fluorine. All powders were weighed according to the designed composition, and ground thoroughly. The mixture was sintered in an alumina crucible using the following profile: heat to 800℃ at 3℃ / min and hold for 5h; then heat to 1100℃ and hold for 7h; finally cool naturally to room temperature. This procedure was repeated to prepare batches with different Zr concentrations.

Crystal growth

Crystal growth was carried out using a self-designed modified crucible lowering furnace, and the temperature was controlled by a VBF1600 high-temperature vertical lowering furnace control system manufactured by Shanghai Jingcui Materials Technology Co., Ltd. (China). Polycrystalline charges with different Zr concentrations were loaded into platinum crucibles that had been cleaned with hydrochloric acid and sealed. Rounded seed crystals were placed at the bottom of each crucible. The crucibles were then inserted into insulating tubes filled with alumina powder. Temperature was monitored by thermocouples, and the seed melt interface was aligned with the lower thermocouple for accurate control. The assembly was placed in the growth furnace, and the temperature was set to 1320℃ so that the seeding region lay within the axial gradient. After complete melting, the crucibles were lowered at 0.2–0.3 mm/h for 20 days. The crystals were then cooled to room temperature at ≤ 40℃/h, held for 48h, and removed, yielding

three 1 inch diameter crystals with different Zr contents. Finally, the crystals were poled at 1190℃ under a current density of 7 mA / cm^2 for 60 min to obtain a single domain state.After annealing and poling, the crystals were cut into thin slices of 1.0 mm and 3.0 mm thickness and polished to optical grade for various performance tests.

Powder X-ray diffraction

Powder X-ray diffraction (XRD) patterns were collected using a TD-3500 diffractometer with Kα radiation (λ = 0.15406 nm). Data were acquired over 10–80° at an operating voltage of 10 kV and a current of 5 mA. The X-ray diffraction patterns of LN: Zr,U polycrystalline powder were shown in Figure S1.

Crystalline quality

The X-ray rocking curve of Bruker HRXRD-5000 was used to test 1.0 mm thick samples to characterize the crystalline quality of LN:Zr,U crystals. The rocking curves were shown in Figure S3.

X-ray photoelectron spectroscopy

X-ray photoelectron spectroscopy (XPS) measurements were performed using a Thermo Scientific K-Alpha+ spectrometer (USA) equipped with an Al Kα monochromated micro-focused X-ray source. The spot size could be continuously adjusted from 30 to 400 μm with a step size of 5 μm. After charge correction referencing the adventitious C1s peak, the spectra were deconvoluted by peak fitting using the XPS-PEAKS software. The chemical states of the elements were determined by analyzing the binding energies of the fitted peaks.The XPS spectra of LN:Zr,U and the fitting peaks by the XPS peaks software were shown in Figure S4.

UV–Visible absorption spectra

UV–Visible absorption spectra of the LN:Zr,U crystals were measured at room temperature using a Cary-5000 spectrophotometer. The wavelength range was 300–800 nm with a step size of 0.5 nm.

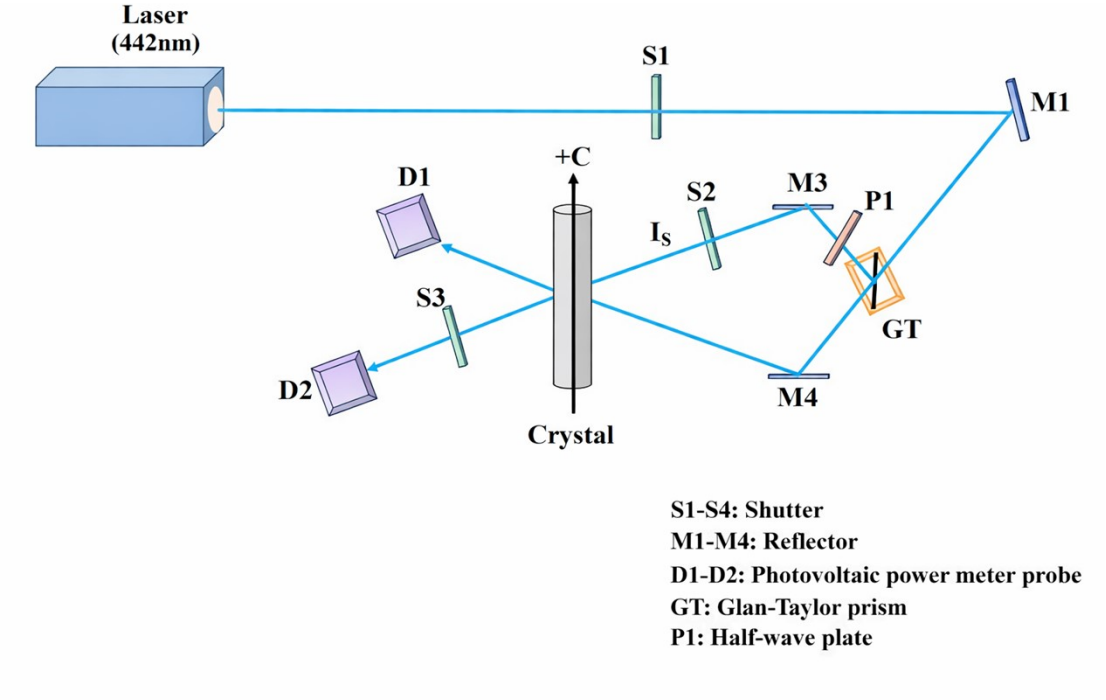

Figure S1. Schematic drawing of the two-beam coupling experiment.

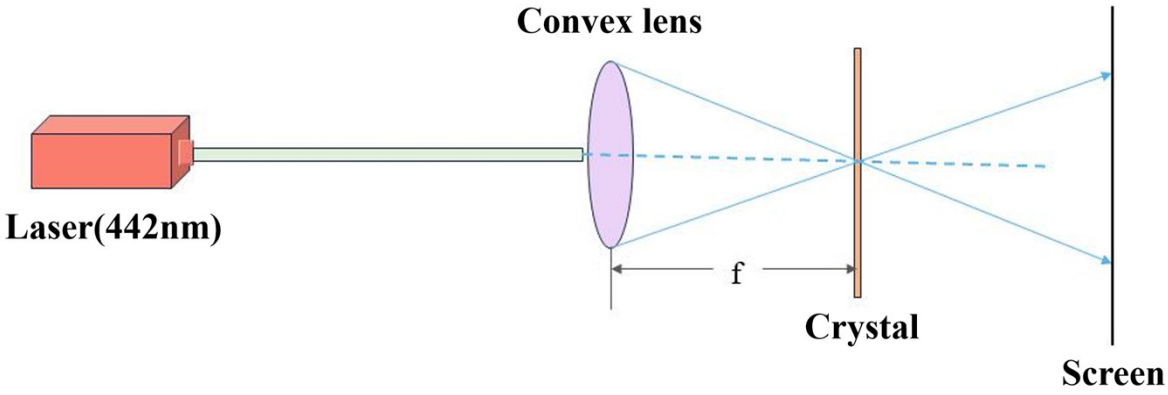

Figure S2. Schematic drawing of the optical damage resistance experiment.

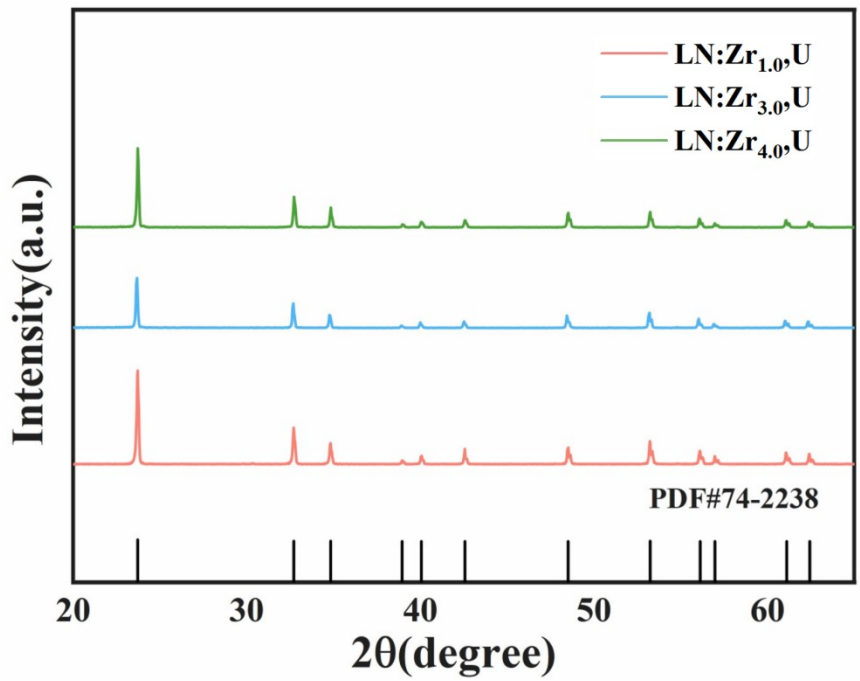

Figure S3. The X-ray diffraction patterns of LN: Zr,U polycrystalline powder.

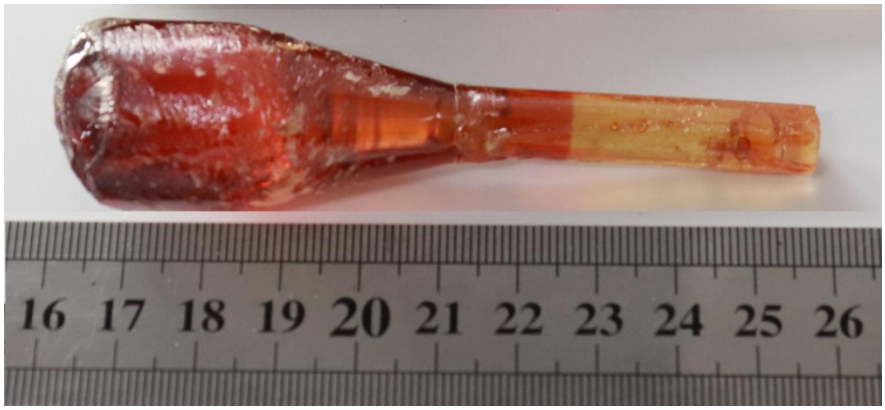

Figure S4. LN:Zr,U crystal was grown by the modified vertical Bridgman method.

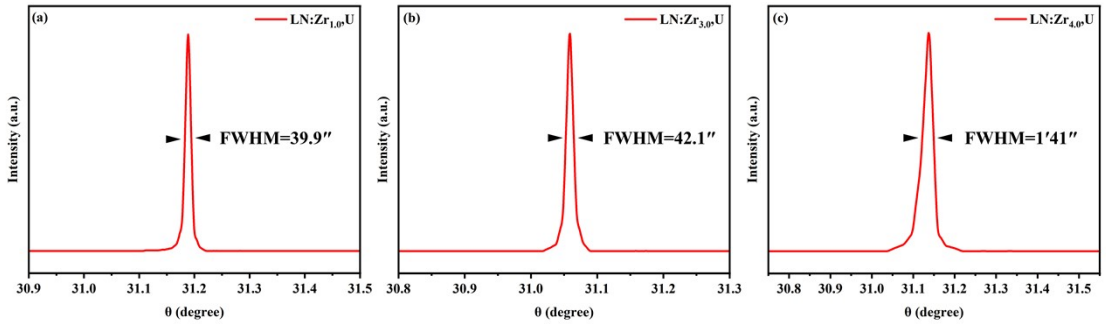

Figure S5. X-ray rocking curves of LN:Zr,U crystals in (001) direction.(a) LN: $Zr_{1.0}$,U, (b) LN: $Zr_{3.0}$,U, (c) LN: $Zr_{4.0}$,U.

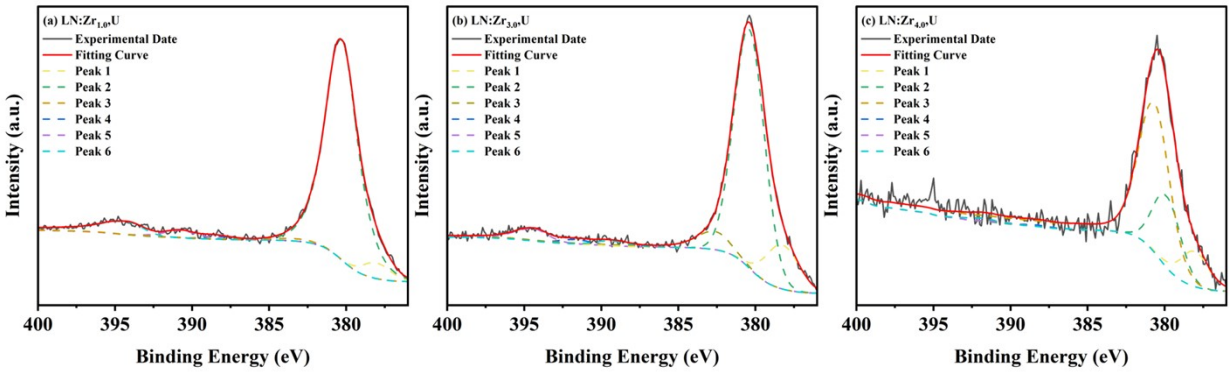

Figure S6. The XPS spectra of LN:Zr,U and the fitting peaks by the XPS peaks software.

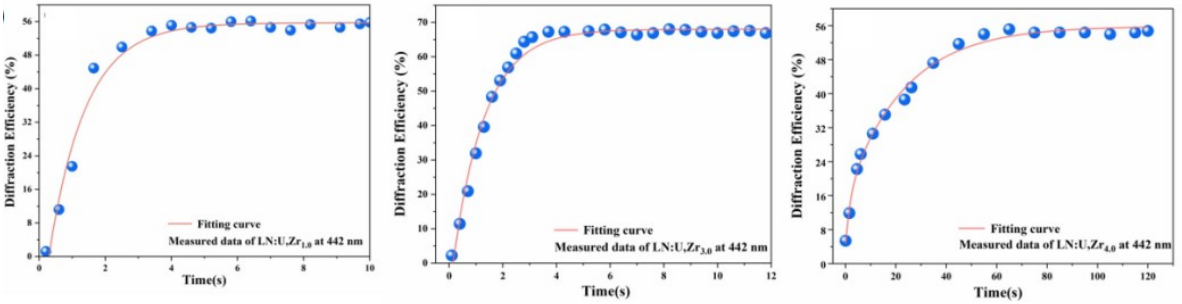

Figure S7. The holographic writing curves of LN:Zr,U crystals at 442 nm. (a) LN: $Zr_{1.0}$,U,(b) LN: $Zr_{3.0}$,U,(c) LN: $Zr_{4.0}$,U.

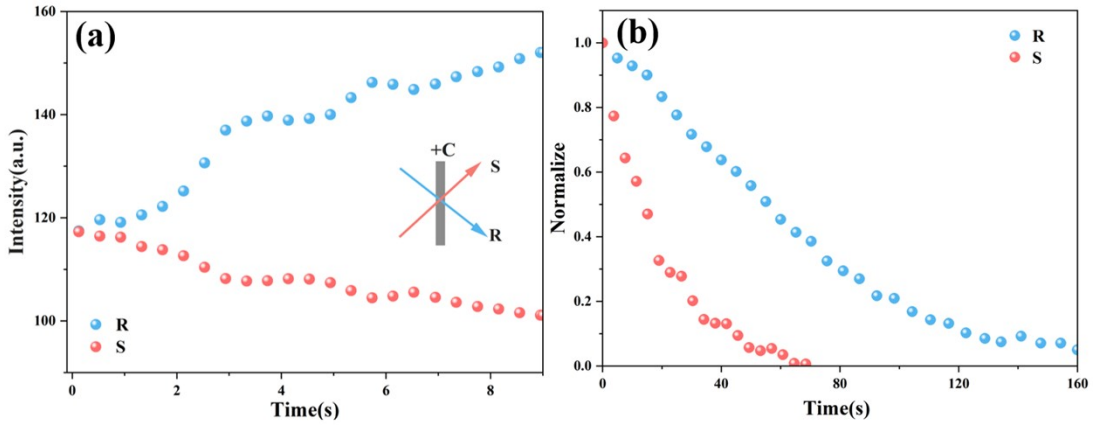

Figure S8. Two-beam coupling measurements at 442 nm (a) energy transfer curve of LN:$Zr_{1.0}$,U. (b) grating erasure curves of LN:$Zr_{1.0}$,U.

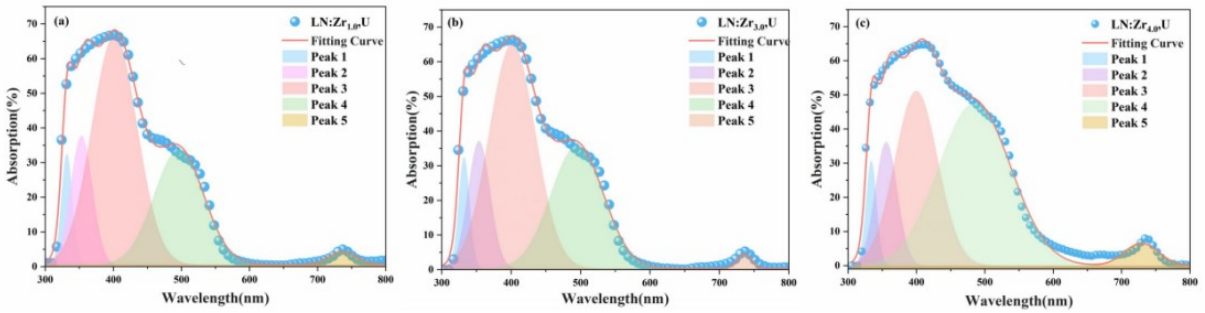

Figure S9. (a) Absorption difference of LN: $Zr_{1.0}$,U relative to CLN. (b) Absorption difference of LN: $Zr_{3.0}$,U relative to CLN. (c) Absorption difference of LN: $Zr_{4.0}$,U relative to CLN.

Table S1. Comparison of the nominal and actual dopant concentrations of different elements in LN:Zr, U

Sample	LN: $Zr_{1.0}$,U		LN: $Zr_{3.0}$,U		LN: $Zr_{4.0}$,U	
Element	Zr	U	Zr	U	Zr	U
Nominal concentration in the starting composition (mol%)	1.0	0.6	3.0	0.6	4.0	0.6
ICP-measured concentration in the grown crystal(mol%)	1.17	0.589	3.062	0.581	3.815	0.531

Table S2. XPS fitting results for LN:Zr,U crystals.

Samples	Ions	U4f7/2				U4f5/2			
		Position (eV)	FWHM	Peak area fractions (CPS • eV)	Atomic%	Position (eV)	FWHM	Peak area fractions (CPS • eV)	Atomic%
LN:U,$Zr_{1.}$	U^{4+}	378.01(±0.50)	2.13	2458.43	4.56	388.31(±0.50)	2.13	420.11	1.00

	U^{5+} 380.28(±0.50)	2.49	42508.80	79.02	390.72(±0.50)	2.49	1435.43	3.41
	U^{6+} 382.96(±0.50)	2.50	938.52	1.75	394.26(±0.50)	2.50	4308.20	10.26
	U^{4+} 378.24(±0.50)	2.50	8208.01	13.50	389.31(±0.50)	2.50	887.16	1.87
LN:U,$Zr_{3.0}$	U^{5+} 380.41(±0.50)	2.34	41799.18	68.87	391.71(±0.50)	2.34	764.55	1.61
	U^{6+} 382.57(±0.50)	2.23	4953.00	8.17	394.37(±0.50)	2.23	2832.99	5.98
	U^{4+} 378.01(±0.50)	2.16	1830.88	10.79	388.31(±0.50)	2.16	78.97	0.59
LN:U,$Zr_{4.0}$	U^{5+} 379.84(±0.50)	2.12	3502.02	20.67	390.28(±0.50)	2.12	47.14	0.36
	U^{6+} 380.65(±0.50)	2.38	11208.23	66.20	391.95(±0.50)	2.38	183.77	1.39

Table S3. Fitting results from the difference absorption spectra of LN:Zr,U crystals.

Crystal	Peak1(nm)	Peak2(nm)	Peak3(nm)	Peak4(nm)	Peak5(nm)
LN:$Zr_{1.0}$,U	331.72	353.17	401.63	496.17	736.67
LN:$Zr_{3.0}$,U	332.29	353.79	401.66	494.91	735.95
LN:$Zr_{4.0}$,U	333.92	355.77	399.81	484.96	729.06